Hindawi Publishing Corporation
International Journal of Photoenergy
Volume 2012, Article ID 593245, 6 pages
doi:10.1155/2012/593245

*Research Article*

# Enhanced Visible Light Photocatalytic Activity of Mesoporous Anatase $TiO_2$ Codoped with Nitrogen and Chlorine

**Xiuwen Cheng,[1,2,3] Xiujuan Yu,[1,2] Zipeng Xing,[1,2] and Lisha Yang[1,2]**

[1] *Department of Environmental Science and Engineering, Heilongjiang University, Xuefu Road 74, Nangang District, Harbin 150080, China*
[2] *Key Laboratory of Chemical Engineering Process & Technology for High-Efficiency Conversion, College of Heilongjiang Province, Harbin 150080, China*
[3] *State Key Laboratory of Urban Water Resources and Environment (SKLUWRE), Department of Environmental Science and Engineering, Harbin Institute of Technology, Huanghe Road 73, Nangang District, Harbin 150090, China*

Correspondence should be addressed to Xiujuan Yu, yuxjuan@hit.edu.cn

Received 26 November 2011; Revised 10 December 2011; Accepted 10 December 2011

Academic Editor: Jiaguo Yu



Anatase mesoporous titanium dioxide codoped with nitrogen and chlorine (N-Cl-$TiO_2$) photocatalysts were synthesized through simple one-step sol-gel reactions in the presence of ammonium chloride. The resulting materials were characterized by X-ray diffraction (XRD), transmission electron microscope (TEM), X-ray photoelectron spectroscopy (XPS), and ultraviolet-visible diffuse reflection spectrum (UV-vis DRS). XRD results indicated that codoping with nitrogen and chlorine could effectively retard the phase transformation of $TiO_2$ from anatase to rutile and the growth of the crystallite sizes. XPS revealed that nitrogen and chlorine elements were incorporated into the lattice of $TiO_2$ through substituting the lattice oxygen atoms. DRS exhibited that the light absorption of N-Cl-$TiO_2$ in visible region was greatly improved. As a result, the band gap of $TiO_2$ was reduced to 2.12 eV. The photocatalytic activity of the as-synthesized $TiO_2$ was evaluated for the degradation of RhB and phenol under visible light irradiation. It was found that N-Cl-$TiO_2$ catalyst exhibited higher visible light photocatalytic activity than that of P25 $TiO_2$ and N-$TiO_2$, which was attributed to the small crystallite size, intense light absorption in visible region, and narrow band gap.

## 1. Introduction

Titanium dioxide ($TiO_2$) is known as a semiconductor with various kinds of application in solar energy conversion, gas sensors, air purification, and waste water treatment due to its cheapness, nontoxicity, and strong oxidation power [1–6]. However, anatase $TiO_2$ can only be excited by UV light with wavelengths less than 388 nm, which only accounts for a small part of the solar spectrum [7]. In order to effectively extend the light absorption to visible region and enhance the photocatalytic activity, many attempts have been made, such as dye sensitization, noble metal deposition, coupling of $TiO_2$ with a narrow semiconductor and doping of $TiO_2$ with foreign ions. Among these, doping of $TiO_2$ with foreign ions has been an effective and feasible approach to improve the visible light response and photocatalytic activity [8–13]. Recently, many researches indicate that $TiO_2$ doping with two different species into the lattice could further enhance the visible light photocatalytic activity. Sun et al. [14] synthesized C-S-codoped $TiO_2$ by the hydrolysis of tetrabutyl titanate in a mixed aqueous solution containing thiourea and urea. Lv et al. [15] prepared C-N-codoped $TiO_2$ nanoparticles with visible light photocatalytic activity. Xu and Zhang [16] reported an enhanced photocatalytic activity of the C-Cl-codoped $TiO_2$ powders towards the degradation of RhB under visible light irradiation. Although such reports demonstrated successful fabrication of relative high photocatalytic activity, they still suffered from some deficiencies due to the discharge of poisonous gases, troublesome procedure during the reaction process.

In this study, N-Cl-codoped $TiO_2$ photocatalyst (N-Cl-$TiO_2$) has been synthesized through simple one-step sol-gel reactions in the presence of ammonium chloride. N and Cl elements were incorporated into the lattice of $TiO_2$ through

substituting the lattice oxygen atoms. As expected, the N-Cl-codoped $TiO_2$ catalyst exhibited higher visible light response and photocatalytic activity than that of P25 $TiO_2$ and N-$TiO_2$. Further, the activity-enhanced mechanism was also discussed in detail.

## 2. Experimental

*2.1. Synthesis of Materials.* Typically, a solution consisting of 10 mL absolute EtOH, 12 mL dilute $HNO_3$ (1 : 5, volume ratio between $HNO_3$ and DI water), and the desired amount of ammonium chloride was added dropwise into a solution containing 40 mL absolute EtOH and 10 mL $Ti(OBu)_4$ within 120 min under vigorous stirring. After being aged for 6 h at room temperature, the $TiO_2$ precursor was received by drying the wet gel in an oven for 36 h. Finally, the N-Cl-codoped $TiO_2$ sample was obtained by calcining the precursor at 623 K for 4 h with a heating rate of $3\,K\cdot min^{-1}$. For comparison, pure $TiO_2$ and N-$TiO_2$ catalysts were synthesized as the reference according to the previous work of our groups [17].

*2.2. Characterization of Materials.* X-ray diffraction (XRD) patterns were collected on Model D/MAX-IIIB diffractometer equipped with Cu K$\alpha$ radiation source ($\lambda = 0.15406$ nm). An accelerating voltage of 40 kV and an emission current of 30 mA with a scanning rate of $5^\circ\cdot min^{-1}$ were employed, respectively. Transmission electron microscopy (TEM) was taken on a JEOL JEM-2010 EX instrument operated at an accelerating voltage of 200 kV. High-resolution transmission electron micrograph (HRTEM) was obtained by employing a FEI TECNAI G2 S-TWIN with a 200 kV accelerating voltage. X-ray photoelectron spectroscopy (XPS) was performed on a Model PHI-5700 ESCA apparatus with Al K$\alpha$ X-ray source. All the binding energies (BE) were referenced with the adventitious carbon (binding energy = 284.6 eV). The ultraviolet-visible diffuse reflectance spectroscopy (UV-vis DRS) of the as-synthesized $TiO_2$ samples was recorded with a Model Shimadzu UV-2550 spectrophotometer.

*2.3. Evaluation of Photocatalytic Activity.* The experiments were carried out in a 100 mL quartz photochemical reactor and the visible light source was provided from a side of the reactor, by a 350 W Xe-arc lamp equipped with a UV-cutoff filter ($\lambda > 420$ nm). In each run, 20 mg $TiO_2$ catalyst was added into 20 mL RhB solution of $10\,mg\cdot L^{-1}$. Prior to photoreaction, the solution was magnetically stirred in the dark for 30 min to establish the equilibrium of adsorption-desorption. At given time intervals, the samples after filtration and centrifugation were analyzed by a T6 UV-vis spectrometer. In addition, the photodegradation of uncolored phenol was similar to that of RhB, and the concentration was determined by the colorimetric method of 4-aminoantipyrine at the wavelength of 510 nm.

## 3. Results and Discussion

*3.1. XRD and TEM Analysis.* Figure 1 showed the XRD patterns of the pure and N-Cl-codoped $TiO_2$ samples. It can

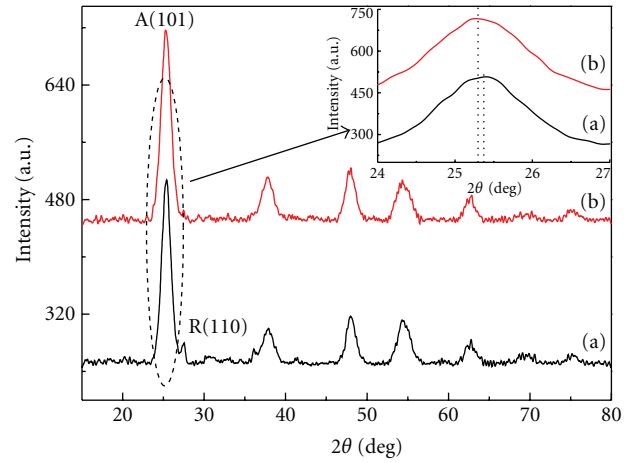


Figure 1: XRD patterns of pure (a) and N-Cl-doped (b) $TiO_2$ photocatalysts.

be seen that pure $TiO_2$ contained anatase (JCPDS. No 21–1272) and trace of rutile (JCPDS. No 21–1276). However, N-Cl-$TiO_2$ consisted of anatase as a unique phase (JCPDS. No 21–1272), indicating that codoping with nitrogen and chlorine could effectively retard the formation of rutile. In addition, no XRD peaks relate to the dopants were detected. One reason was that the concentration of the dopants was so low that it cannot be detected by XRD. The other was that the dopants were incorporated into the lattice of $TiO_2$ through substituting oxygen atoms or located in the interstitial sites. Further, as seen from the inset of Figure 1, the diffraction peak position of N-Cl-codoped $TiO_2$ shifted to lower angle in comparison with the pure $TiO_2$, suggesting that oxygen atoms in the lattice of anatase in codoped $TiO_2$ sample may be substituted by the dopants. Further, the average crystallite sizes of the as-synthesized samples can be calculated by applying the Debye-Scherrer formula [18] on the anatase (101) diffraction peaks:

$$d = \frac{K\lambda}{\beta\cos\theta}, \tag{1}$$

where $d$ is the crystallite size, $\lambda$ is the wavelength of X-ray radiation (in our test, $\lambda = 0.15418$ nm), K is a constant ($K = 0.89$), $\beta$ is the full width at half-maximum, and $\theta$ is the diffraction angle. The calculated $d$ values were 10 and 5 nm for pure and N-Cl-codoped $TiO_2$, respectively. Thus, we can conclude that codoping with N and Cl elements could effectively retard the phase transformation of $TiO_2$ from anatase to rutile and growth of the crystallite size.

The crystal structure and grain size of N-Cl-codoped $TiO_2$ sample were also evaluated with TEM and HRTEM. Figure 2 showed the TEM and HRTEM images of mesoporous N-Cl-$TiO_2$ photocatalyst. As shown in Figure 2(a), many spherical aggregates of nanoparticles were observed with the nanoparticles at about 5~10 nm in crystallite sizes. However, an obvious agglomerative phenomenon was observed. As shown in Figure 2(b), the lattice fringes of nanocrystals revealed the lattice spacing of 0.352 nm, which

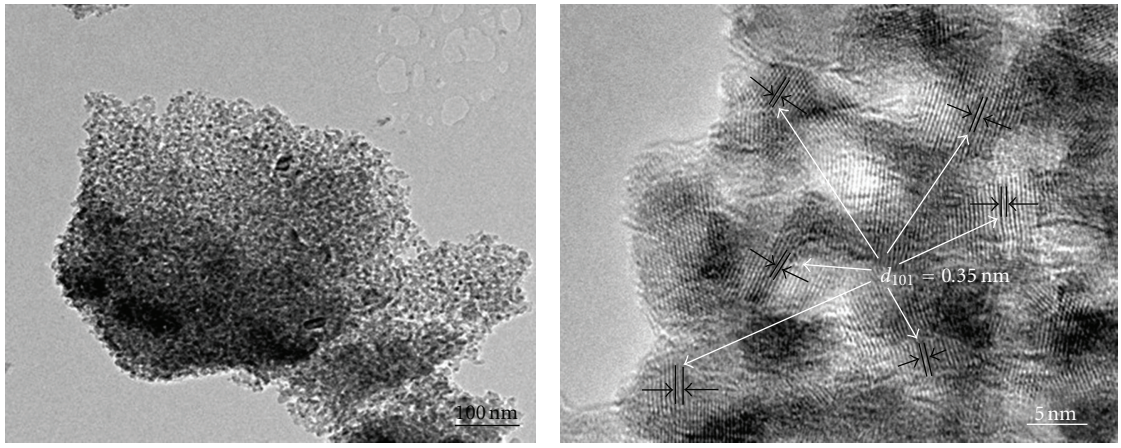


(a) (b)

Figure 2: TEM (a) and HRTEM (b) images of N-Cl-codoped $TiO_2$ photocatalyst.

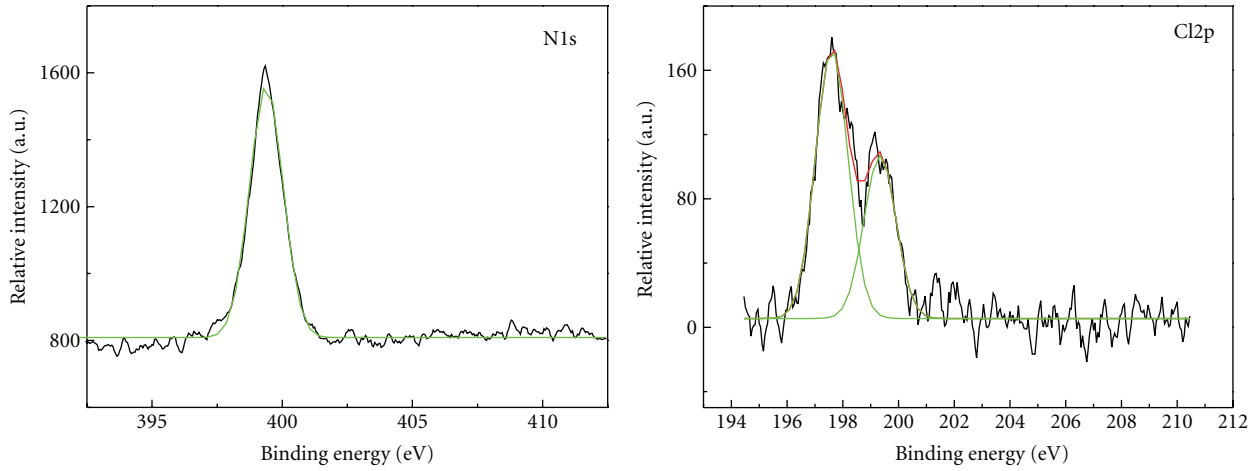


(a) (b)

Figure 3: High-resolution XPS spectra of N1*s* (a) and Cl2*p* (b) for N-Cl-codoped $TiO_2$ photocatalyst.

was in good accordance with the anatase (101) lattice fringes of 0.352 nm [19].

*3.2. XPS Analysis.* In order to investigate the chemical states of the N-Cl-codoped $TiO_2$ sample, XPS was conducted and shown in Figure 3. As seen from Figure 3(a), a single peak at binding energy of 399.6 eV was observed, which was attributed to the presence of substitutional N in O–Ti–N bond [20, 21], indicating that some lattice oxygen were substituted by nitrogen atoms, which correlated with the visible light photocatalytic activity of doped $TiO_2$. As shown in Figure 3(b), two peaks at 197.7 and 199.3 eV seen from the Cl2p core-level XPS spectrum were observed. The strong peak at 197.7 eV was assigned to $Cl^-$ ions physically adsorbed on the surface of codoped $TiO_2$ [22], while the minor peak located at 199.3 eV might be assigned to the Cl incorporated into the lattice of $TiO_2$ [16], indicating that nitrogen and chlorine were incorporated into the lattice of $TiO_2$ through substituting the lattice oxygen atoms.

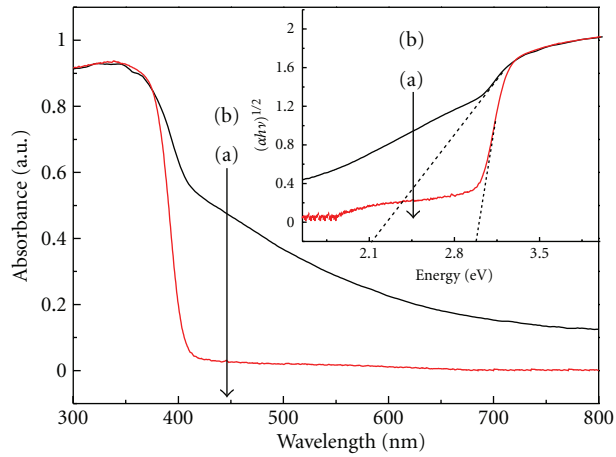


Figure 4: UV-vis DRS of the pure (a) and N-Cl-codoped (b) $TiO_2$ photocatalysts.

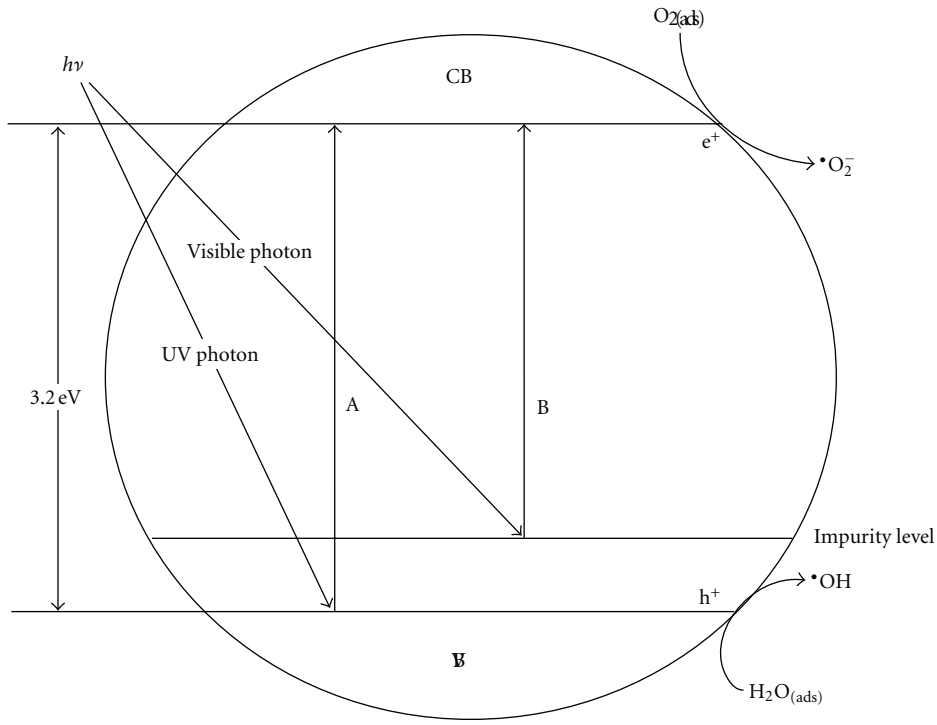


Figure 5: Scheme of photocatalytic mechanism of N-Cl-codoped-$TiO_2$ photocatalyst.

*3.3. DRS Analysis.* Generally speaking, narrower band gap of a semiconductor corresponds to a higher photocatalytic activity. In order to investigate the optical absorbance property of pure and N-Cl-codoped $TiO_2$ samples, ultraviolet-visible diffuse reflection spectra were conducted and shown in Figure 4. In addition, band gap energies were also calculated according to the Kubelka-Munk function [23], which was shown in the insert in Figure 4. Noticeably, both as-synthesized $TiO_2$ samples showed a typical absorbance spectrum with an intense transition in the UV region of the spectra, corresponding to the band gap energy of 3.2 eV from the intrinsic band gap of pure anatase. However, the light absorption edge of N-Cl-codoped $TiO_2$ sample was greatly red-shifted to the visible light region, demonstrating a decrease in the band gap energy, which was responsible for the impurity level (formed from hybridization of N2p and Cl2p levels) in the band gap of $TiO_2$. After calculating, the band gap energy of N-Cl-codoped $TiO_2$ was 2.12 eV. As a result, the N-Cl-codoped $TiO_2$ should most probably possess excellent visible light photocatalytic activity for organic degradation.

*3.4. Mechanism Analysis.* Based on the above analysis, a possible photocatalytic mechanism was proposed and shown in Figure 5. Nitrogen and chlorine were incorporated into the lattice of $TiO_2$ through substituting lattice oxygen atoms. Thus, a new impurity level was formed from the hybridization of N2p and Cl2p levels between the valence band and conduction band of $TiO_2$. As shown in Figure 5, pure $TiO_2$ exhibited a relatively low visible photocatalytic activity for the degradation of pollutants due to its wide band gap (3.2 eV, process A). After codoping with nitrogen and chlorine elements, electrons can be promoted from the impurity level to the conduction band of $TiO_2$ (process B), thereby enhancing the separation efficiency of photoinduced charge carriers. As a result, more departed photoinduced electrons and holes can participate in the photocatalytic reactions. Further, the process of visible light photocatalytic oxidation of phenol can be described as followed

Firstly, electrons and holes were generated under visible irradiation.

$$\text{N-Cl-TiO}_2 + h\nu \longrightarrow h_{VB}^{+} + e_{CB}^{-} \tag{2}$$

Then, the departed electrons and holes can react with the absorbed $O_2$ and $H_2O$ molecules, respectively, forming the main active species (such as $\cdot O_2^-$ and $\cdot OH$) responsible for the degradation of organic pollutants, such as RhB and phenol in our case. Eventually, organic pollutants were mineralized into small molecules, such as $CO_2$ and $H_2O$

$$\begin{aligned} O_{2(ads)} + e_{CB}^{-} &\longrightarrow \cdot O_2^{-} \\ h_{VB}^{+} + H_2O_{(ads)} &\longrightarrow \cdot OH + H+ \\ \cdot O_2^{-} + 2H^{+} + e_{CB}^{-} &\longrightarrow \cdot OH + OH^{-} \\ h_{VB}^{+} + OH^{-} &\longrightarrow \cdot OH \\ \cdot OH + \text{Organic} &\longrightarrow \cdots \longrightarrow CO_2 + H_2O \end{aligned} \tag{3}$$

*3.5. Photocatalytic Activity.* The photocatalytic activities of the $TiO_2$ samples were evaluated by photocatalytic degradation of RhB and phenol under visible light irradiation.

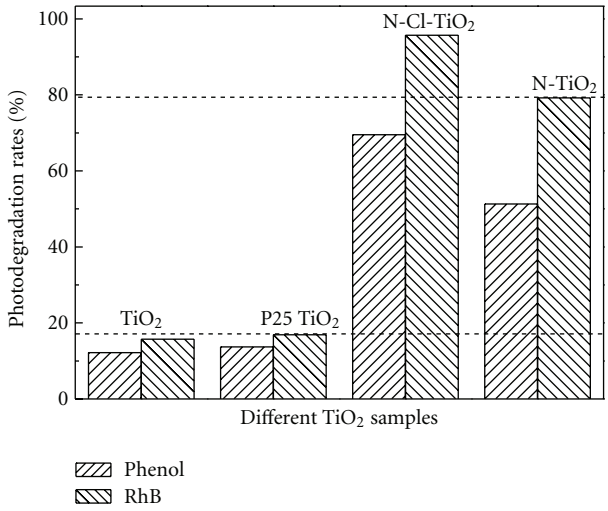


Figure 6: Photocatalytic degradation rates of RhB and phenol on different $TiO_2$ samples.

Figure 6 showed the photocatalytic degradation rates of RhB and phenol on different $TiO_2$ samples. As a comparison, the photocatalytic activity of P25 $TiO_2$ and N-$TiO_2$ was also measured and shown in Figure 6. As seen from Figure 6, N-Cl-codoped $TiO_2$ sample exhibited higher photocatalytic activities than that of P25 $TiO_2$ and N-$TiO_2$ catalysts, suggesting that the visible-induced photocatalytic reactions can contribute to the degradation of the colored RhB and uncolored phenol. Under the visible light irradiation for 120 min, 95.7% and 82% degradation rates could be achieved for colored RhB and uncolored phenol, respectively. The enhanced photocatalytic activity of N-Cl-codoped $TiO_2$ was attributed to the small crystallite size, intense light absorption in visible region, and narrow band gap energy.

## 4. Conclusions

Based on the above analysis, the following conclusions can be drawn: (1) N-Cl-codoped $TiO_2$ catalyst with high visible light photocatalytic activity has been successfully synthesized through simple one-step sol-gel reactions in the presence of ammonium chloride. (2) $TiO_2$ codoping with N and Cl could effectively retard the phase transformation of $TiO_2$ from anatase to rutile and growth of crystallite size. (3) N and Cl elements were incorporated into the lattice of $TiO_2$ through substituting some oxygen atoms, which could form a new impurity level between the valence band and conduction band of $TiO_2$. (4) Codoping with N and Cl could greatly improve the photoresponse of $TiO_2$, thereby reducing the band gap. (5) The enhanced activity of N-Cl-codoped $TiO_2$ was mainly attributed to the small crystallize size, intense light absorption in visible region, and narrow band gap.

## Acknowledgments

The authors wish to gratefully acknowledge the financial support by National Natural Science Foundation of China for Youth (21106035) and Youth Scholar Backbone Supporting Plan Project for general colleges and universities of Heilongjiang province (1151G034).

## References

[1] J. Gamage and Z. Zhang, "Applications of photocatalytic disinfection," *International Journal of Photoenergy*, vol. 2010, Article ID 764870, 11 pages, 2010.

[2] M. Grätzel, "Photoelectrochemical cells," *Nature*, vol. 414, no. 6861, pp. 338–344, 2001.

[3] M. Andersson, L. Österlund, S. Ljungström, and A. Palmqvist, "Preparation of nanosize anatase and rutile $TiO_2$ by hydrothermal treatment of microemulsions and their activity for photocatalytic wet oxidation of phenol," *Journal of Physical Chemistry B*, vol. 106, no. 41, pp. 10674–10679, 2002.

[4] J. Yu, L. Qi, and M. Jaroniec, "Hydrogen production by photocatalytic water splitting over Pt/$TiO_2$ nanosheets with exposed (001) facets," *Journal of Physical Chemistry C*, vol. 114, no. 30, pp. 13118–13125, 2010.

[5] J. Anthony, P. A. Fernandez-Ibañez, P. S. M. Dunlop, D. M. A. Alrousan, and J. W. J. Hamilton, "Photocatalytic enhancement for solar disinfection of water: a review," *International Journal of Photoenergy*, vol. 2011, Article ID 798051, 12 pages, 2011.

[6] Y. Zhu, J. Shi, Z. Zhang, C. Zhang, and X. Zhang, "Development of a gas sensor utilizing chemiluminescence on nanosized titanium dioxide," *Analytical Chemistry*, vol. 74, no. 1, pp. 120–124, 2002.

[7] S.-K. Joung, T. Amemiya, M. Murabayashi, and K. Itoh, "Relation between photocatalytic activity and preparation conditions for nitrogen-doped visible light-driven $TiO_2$ photocatalysts," *Chemistry*, vol. 12, pp. 5526–5534, 2006.

[8] A. Solbrand, A. Henningsson, S. Södergren, H. Lindström, A. Hagfeldt, and S. E. Lindquist, "Charge transport properties in dye-sensitized nanostructured $TiO_2$ thin film electrodes studied by photoinduced current transients," *Journal of Physical Chemistry B*, vol. 103, no. 7, pp. 1078–1083, 1999.

[9] M. Zhou, J. Yu, and B. Cheng, "Effects of Fe-doping on the photocatalytic activity of mesoporous $TiO_2$ powders prepared by an ultrasonic method," *Journal of Hazardous Materials*, vol. 137, no. 3, pp. 1838–1847, 2006.

[10] R. Asahi, T. Morikawa, T. Ohwaki, K. Aoki, and Y. Taga, "Visible-light photocatalysis in nitrogen-doped titanium oxides," *Science*, vol. 293, no. 5528, pp. 269–271, 2001.

[11] M. Bowker, P. Stone, R. Bennett, and N. Perkins, "Formic acid adsorption and decomposition on $TiO_2$(1 1 0) and on Pd/$TiO_2$(1 1 0) model catalysts," *Surface Science*, vol. 511, no. 1-3, pp. 435–448, 2002.

[12] J. Yu, Q. Xiang, and M. Zhou, "Preparation, characterization and visible-light-driven photocatalytic activity of Fe-doped titania nanorods and first-principles study for electronic structures," *Applied Catalysis B*, vol. 90, no. 3-4, pp. 595–602, 2009.

[13] S. Kohtani, A. Kudo, and T. Sakata, "Spectral sensitization of a $TiO_2$ semiconductor electrode by CdS microcrystals and its photoelectrochemical properties," *Chemical Physics Letters*, vol. 206, no. 1-4, pp. 166–170, 1993.

[14] H. Sun, Y. Bai, Y. Cheng, W. Jin, and N. Xu, "Preparation and characterization of visible-light-driven carbon—sulfur-codoped $TiO_2$ photocatalysts," *Industrial and Engineering Chemistry Research*, vol. 45, no. 14, pp. 4971–4976, 2006.

[15] K. Lv, H. Zuo, J. Sun et al., "(Bi, C and N) codoped $TiO_2$ nanoparticles," *Journal of Hazardous Materials*, vol. 161, no. 1, pp. 396–401, 2009.

[16] H. Xu and L. Zhang, "Controllable one-pot synthesis and enhanced visible light photocatalytic activity of tunable C-Cl-Codoped $TiO_2$ nanocrystals with high surface area," *Journal of Physical Chemistry C*, vol. 114, no. 2, pp. 940–946, 2010.

[17] Y. Q. Wang, X. J. Yu, and D. Z. Sun, "Synthesis, characterization, and photocatalytic activity of $TiO_2$-xNx nanocatalyst," *Journal of Hazardous Materials*, vol. 144, no. 1-2, pp. 328–333, 2007.

[18] Q. Zhang, L. Gao, and J. Guo, "Effects of calcination on the photocatalytic properties of nanosized $TiO_2$ powders prepared by $TiCl_4$ hydrolysis," *Applied Catalysis B*, vol. 26, no. 3, pp. 207–215, 2000.

[19] W. Zhou, F. Sun, K. Pan et al., "Well-ordered large-pore mesoporous anatase $TiO_2$ with remarkably high thermal stability and improved crystallinity: preparation, characterization, and photocatalytic performance," *Advanced Functional Materials*, vol. 21, no. 10, pp. 1922–1930, 2011.

[20] J. H. Xu, J. Li, W. L. Dai, Y. Cao, H. Li, and K. Fan, "Simple fabrication of twist-like helix N,S-codoped titania photocatalyst with visible-light response," *Applied Catalysis B*, vol. 79, no. 1, pp. 72–80, 2008.

[21] Y. Cong, J. Zhang, F. Chen, and M. Anpo, "Synthesis and characterization of nitrogen-doped $TiO_2$ nanophotocatalyst with high visible light activity," *Journal of Physical Chemistry C*, vol. 111, no. 19, pp. 6976–6982, 2007.

[22] H. Xu and L. Zhang, "Selective nonaqueous synthesis of C-Cl-codoped $TiO_2$ with visible-light photocatalytic activity," *Journal of Physical Chemistry C*, vol. 114, no. 26, pp. 11534–11541, 2010.

[23] F. Spadavecchia, G. Cappelletti, S. Ardizzone et al., "Solar photoactivity of nano-N-$TiO_2$ from tertiary amine: role of defects and paramagnetic species," *Applied Catalysis B*, vol. 96, no. 3-4, pp. 314–322, 2010.